

AN ADAPTIVE RANDOM BIT MULTILEVEL ALGORITHM FOR SDES

MICHAEL B. GILES, MARIO HEFTER, LUKAS MAYER, AND KLAUS RITTER

ABSTRACT. We study the approximation of expectations $E(f(X))$ for solutions X of stochastic differential equations and functionals f on the path space by means of Monte Carlo algorithms that only use random bits instead of random numbers. We construct an adaptive random bit multilevel algorithm, which is based on the Euler scheme, the Lévy-Ciesielski representation of the Brownian motion, and asymptotically optimal random bit approximations of the standard normal distribution. We numerically compare this algorithm with the adaptive classical multilevel Euler algorithm for a geometric Brownian motion, an Ornstein–Uhlenbeck process, and a Cox-Ingersoll-Ross process.

1. INTRODUCTION

We study the approximation of expectations $E(f(X))$, where $X = (X(t))_{t \in [0,1]}$ is the r -dimensional solution of an autonomous stochastic differential equation (SDE) driven by a d -dimensional Brownian motion and where $f: C([0,1], \mathbb{R}^r) \rightarrow \mathbb{R}$ is a functional on the path space. The main contribution of this paper is the construction of an adaptive random bit multilevel algorithm $A_\varepsilon^{\text{bit}}$, which is based on the generic adaptive multilevel algorithm from [5]. Here $\varepsilon > 0$ is an accuracy demand and input to the algorithm, and the maximal level as well as the replication numbers per level are determined adaptively. For a survey on multilevel Monte Carlo algorithms we refer to [4].

The algorithm $A_\varepsilon^{\text{bit}}$ employs the Euler scheme, the Lévy-Ciesielski representation of the Brownian motion (Brownian bridge construction), and the asymptotically optimal random bit approximation of the standard normal distribution according to [7, Thm. 1]. Unfortunately, we have no analysis for the error and the cost of $A_\varepsilon^{\text{bit}}$, and even a proof of the convergence $\lim_{\varepsilon \rightarrow 0} A_\varepsilon^{\text{bit}}(f) = E(f(X))$ (under suitable assumptions on the coefficients of the SDE and the functional f) is missing. Instead we present numerical experiments.

On each level ℓ a multilevel algorithm has to couple a fine approximation and a coarse approximation. In the classical setting, where random numbers are used, one may simply simulate Brownian increments for $2^\ell + 1$ equidistant points. For the fine approximation the Euler scheme with 2^ℓ steps is applied, and for the coarse approximation the step-size is doubled and the corresponding increments are added up. Of course, there are several options for the simulation of the Brownian increments, in particular, one may either simulate the increments directly or use the Lévy-Ciesielski representation of the Brownian motion.

Both of these approaches may be adapted to the random bit setting by approximating all the involved normally distributed random variables by random variables that can be simulated with random bits only. However, in contrast to the classical setting, the two constructions no longer end up in the same distribution. The first approach, where increments are approximated and the approximations are added up, has been presented and analyzed in [6]. Here the random bit approximations of the increments are independent, but an additional bias is introduced, in contrast to the classical setting.

In this paper we present the second approach, which has already been sketched in [4, Sec. 10.2], and which employs the Lévy-Ciesielski representation and random bit approximations to its normally distributed coefficients. Here the approximations of the Brownian increments are no longer independent, which forms an obstacle for an error analysis, but we obtain matching distributions: The distribution of the coarse approximation on level ℓ coincides with the distribution of the fine approximation on level $\ell-1$. Furthermore, this approach is well suited as the building block for an adaptive multilevel algorithm.

In the numerical experiments we apply the adaptive random bit multilevel Euler algorithm $A_\varepsilon^{\text{bit}}$ and the adaptive classical multilevel Euler algorithm A_ε^C , which is based on random numbers, for three processes X and functionals f , namely, the maximum of a geometric Brownian motion and the terminal values of

Date: February 26, 2019.

Key words and phrases. Random bits, multilevel Monte Carlo algorithm, stochastic differential equation, adaption.

an Ornstein–Uhlenbeck process and of a Cox–Ingersoll–Ross process. At first we compare the building blocks, i.e., the random bit Euler scheme and the classical Euler scheme, in terms of their bias and variance decays. The decays depend on the process X and the functional f under consideration, but in all three cases we observe no essential difference between the random bit and the classical Euler scheme. Next we turn to the adaptive algorithms. In all three cases and for both algorithms the actual root mean squared error is almost equal to the accuracy demand ε . Finally, to achieve the same root mean squared error the number of random bits needed by $A_\varepsilon^{\text{bit}}$ is only about 4 to 7 times larger than the number of random numbers needed by A_ε^c .

For the terminal value of the Cox–Ingersoll–Ross process we also apply the truncated Milstein scheme from [9] as the building block, instead of the Euler scheme. This leads to a substantially faster decay of the variance in the classical and in the random bit case. Moreover, the algorithm based on the truncated Milstein scheme and random bits performs as good as the algorithm based on the Euler scheme and random numbers.

2. EULER SCHEMES

Consider an autonomous system

$$dX(t) = a(X(t)) dt + b(X(t)) dW(t), \quad t \in [0, 1],$$

of SDEs with a deterministic initial value $X(0) = x_0 \in \mathbb{R}^r$ and a d -dimensional Brownian motion W , and with drift and diffusion coefficients $a: \mathbb{R}^r \rightarrow \mathbb{R}^r$ and $b: \mathbb{R}^r \rightarrow \mathbb{R}^{r \times d}$, respectively. Furthermore, consider the time discretization given by

$$(1) \quad t_{k,\ell} = k/2^\ell, \quad k = 0, \dots, 2^\ell,$$

together with a suitable choice of

$$(2) \quad V_\ell = (V_{1,\ell}, \dots, V_{2^\ell,\ell})$$

with d -dimensional random vectors $V_{k,\ell}$ on a common probability space. These random vectors are meant to at least approximate the Brownian increments associated to (1), and the corresponding Euler scheme X_ℓ is given by $X_\ell(t_{0,\ell}) = x_0$ and

$$(3) \quad X_\ell(t_{k,\ell}) = X_\ell(t_{k-1,\ell}) + 2^{-\ell} \cdot a(X_\ell(t_{k-1,\ell})) + b(X_\ell(t_{k-1,\ell})) \cdot V_{k,\ell}$$

for $k = 1, \dots, 2^\ell$.

The multilevel approach relies on a coupling of X_ℓ with $\ell \geq 1$ to an Euler scheme $\tilde{X}_{\ell-1}$ with step-size $2^{-(\ell-1)}$. Hence we choose

$$(4) \quad \tilde{V}_{\ell-1} = (\tilde{V}_{1,\ell-1}, \dots, \tilde{V}_{2^{\ell-1},\ell-1})$$

with d -dimensional random vectors $\tilde{V}_{k,\ell-1}$ on the probability space introduced above, and we define, as before, $\tilde{X}_{\ell-1}(t_{0,\ell-1}) = x_0$ and

$$(5) \quad \begin{aligned} \tilde{X}_{\ell-1}(t_{k,\ell-1}) &= \tilde{X}_{\ell-1}(t_{k-1,\ell-1}) + 2^{-(\ell-1)} \cdot a(\tilde{X}_{\ell-1}(t_{k-1,\ell-1})) \\ &\quad + b(\tilde{X}_{\ell-1}(t_{k-1,\ell-1})) \cdot \tilde{V}_{k,\ell-1} \end{aligned}$$

for $k = 1, \dots, 2^{\ell-1}$. Of course, a natural coupling between X_ℓ and $\tilde{X}_{\ell-1}$ is induced by

$$(6) \quad \tilde{V}_{k,\ell-1} = V_{2k,\ell} + V_{2k-1,\ell}, \quad k = 1, \dots, 2^{\ell-1}.$$

Actually, the multilevel approach is based on a hierarchy $V_0, (V_1, \tilde{V}_0), \dots, (V_L, \tilde{V}_{L-1})$ with corresponding Euler schemes, and the following properties are most convenient for its analysis:

- (i) For every $\ell \in \{0, \dots, L\}$ the random vectors $V_{1,\ell}, \dots, V_{2^\ell,\ell}$ are iid with iid real-valued components $V_{k,\ell}^{(1)}, \dots, V_{k,\ell}^{(d)}$.
- (ii) For every $\ell \in \{1, \dots, L\}$ the random vectors $\tilde{V}_{\ell-1}$ and $V_{\ell-1}$ coincide in distribution.

In order to obtain processes with continuous paths we extend X_ℓ and $\tilde{X}_{\ell-1}$ onto $[0, 1]$ by piecewise linear interpolation.

2.1. The Classical Euler Scheme. In the vast majority of papers, $V_{k,\ell}$ and $\tilde{V}_{k,\ell-1}$ are chosen as Brownian increments, i.e.,

$$V_{k,\ell} = W(t_{k,\ell}) - W(t_{k-1,\ell})$$

and

$$\tilde{V}_{k,\ell-1} = W(t_{k,\ell-1}) - W(t_{k-1,\ell-1}),$$

so that we have (6), and (i) and (ii) are satisfied. Error bounds for the Euler scheme w.r.t. various error criteria and under different sets of assumptions concerning the drift and diffusion coefficients are well known in this case. In order to simulate the corresponding distributions a generator for random numbers from $[0, 1]$ has to be available.

2.2. Random Bit Euler Schemes. In the present paper we study the random bit quadrature problem for SDEs, i.e., we consider algorithms that are only allowed to use random bits instead of random numbers, see also [1, 2, 7, 6, 11, 12]. This excludes the use of Brownian increments.

Heuristics and extensive tests for finite precision random bit multilevel algorithms for field programmable gate arrays (FPGAs) are presented in [2, 11, 12]. In [7] the random bit quadrature problem is studied for Gaussian random fields X , and relations to random bit approximation of Gaussian measures are exploited.

Motivated by the weak error analysis of the Euler scheme, the multilevel construction in [1] is based on iid random vectors $V_{1,L}, \dots, V_{2^L,L}$, each of which has iid components $V_{k,L}^{(1)}, \dots, V_{k,L}^{(d)}$ with

$$2^{L/2-1} \cdot V_{1,L}^{(1)} + 1/2 \sim B(1, 1/2).$$

Moreover, the coupling is defined by (6), and (ii) is assumed to hold. It follows that (i) is satisfied as well, and

$$(7) \quad 2^{L/2-1} \cdot V_{1,\ell}^{(1)} + 2^{L-\ell-1} \sim B(2^{L-\ell}, 1/2).$$

See [1, Sec. 3] for error bounds, and [1, Sec. 4.1] for the discussion of fast generation of random quantities in this context.

A different construction is presented and analyzed in [6]. Here the starting point is the approximation of the standard normal distribution based on random bits. Let Φ^{-1} denote the inverse of the distribution function of $N(0, 1)$, and let U be uniformly distributed on

$$(8) \quad D_q = \left\{ \sum_{i=1}^q b_i \cdot 2^{-i} + 2^{-(q+1)} : b_i \in \{0, 1\} \text{ for } i = 1, \dots, q \right\},$$

where $q \in \mathbb{N}$. Obviously, q random bits suffice to simulate the distribution ν_q of $\Phi^{-1} \circ U$, which serves as an approximation of $N(0, 1)$. Further properties of ν_q , in particular, error bounds and the weak asymptotic optimality among all approximations based on q random bits, have been established in [7, Sec. 2.2]. In the construction from [6], (i) is assumed to hold with

$$(9) \quad 2^{\ell/2} \cdot V_{1,\ell}^{(1)} \sim \nu_L,$$

and the coupling is again defined by (6). Consequently, the analogon to (i) also holds for the random vectors $\tilde{V}_{1,\ell-1}, \dots, \tilde{V}_{2^{\ell-1},\ell-1}$, but property (ii) is not satisfied, which introduces an additional bias term in the multilevel analysis. See [6] for error and cost bounds; in particular, a variant of the corresponding multilevel Euler algorithm, which also employs Bakhvalov's trick, is shown to be almost worst case optimal in the class of all Lipschitz continuous functionals $f: C([0, 1], \mathbb{R}^r) \rightarrow \mathbb{R}$ with Lipschitz constant at most one. Observe that the number of random bits that are needed to simulate the distribution of V_ℓ with $\ell = 0$ or the joint distribution of V_ℓ and $\tilde{V}_{\ell-1}$ with $\ell \geq 1$ is of the order $d \cdot L \cdot 2^\ell$.

2.3. The Random Bit Lévy-Ciesielski Euler Scheme. In the sequel we present a new construction of a random bit Euler scheme, which is based on the Lévy-Ciesielski representation of the Brownian motion. Hereby we get matching distributions across the levels in the sense of (ii), but the iid-property (i) is not satisfied. The main advantage of the new construction, compared to the approaches from [1, 6], is that it is well suited as the building block for an adaptive multilevel algorithm.

Consider the sequence of Schauder functions $s^{(i,j)}$ with $i = 0$ and $j = 1$ or $i \in \mathbb{N}$ and $j = 1, \dots, 2^{i-1}$. These functions are given by

$$s^{(i,j)}(t) = \int_0^t h^{(i,j)}(u) \, du, \quad t \in [0, 1],$$

with Haar wavelets $h^{(0,1)} = 1$ and

$$h^{(i,j)} = 2^{(i-1)/2} \cdot (1_{I^{(i,j)}} - 1_{J^{(i,j)}})$$

for $i \in \mathbb{N}$ and $j = 1, \dots, 2^{i-1}$, where

$$I^{(i,j)} = [(j-1)/2^{i-1}, (j-1/2)/2^{i-1}[$$

and

$$J^{(i,j)} = [(j-1/2)/2^{i-1}, j/2^{i-1}[.$$

The Lévy-Ciesielski representation states that

$$(10) \quad W_\ell = s^{(0,1)} \cdot Z^{(0,1)} + \sum_{i=1}^{\ell} \sum_{j=1}^{2^{i-1}} s^{(i,j)} \cdot Z^{(i,j)}$$

with an independent sequence $Z^{(0,1)}, \dots$ of d -dimensional standard normally distributed random vectors converges to a d -dimensional Brownian motion as $\ell \rightarrow \infty$, e.g., in mean square and almost surely w.r.t. the supremum-norm. We add that

$$(11) \quad W_n(t_{k,\ell}) = W_\ell(t_{k,\ell}), \quad k = 0, \dots, 2^\ell,$$

for $\ell, n \in \mathbb{N}_0$ with $\ell < n$. In this sense W_ℓ already yields the values of the Brownian motion at the discretization (1).

In a random bit approximation that corresponds to W_ℓ the number of bits that are spent for the individual terms should depend on i and ℓ , but not on the shift parameter j . We spend

$$q_\ell^{(i)} = 2 \cdot (\ell + 1 - i)$$

random bits for the approximation of the distribution of each of the components of $Z^{(i,j)}$. This choice is motivated by [7, Thm. 2], which determines the weak asymptotics for random bit approximation of a Brownian bridge with respect to the L_2 -norm.

Accordingly, we consider an independent sequence $U_\ell^{(0,1)}, \dots, U_\ell^{(\ell, 2^{\ell-1})}$ of d -dimensional random vectors, with iid components that are uniformly distributed on

$$D_\ell^{(i)} = D_{q_\ell^{(i)}}.$$

To normalize the variances we put

$$\sigma_\ell^{(i)} = 2^{-q_\ell^{(i)}/2} \cdot \left(\sum_{x \in D_\ell^{(i)}} (\Phi^{-1}(x))^2 \right)^{1/2}.$$

Replacing $Z^{(i,j)}$ by

$$Y_\ell^{(i,j)} = 1/\sigma_\ell^{(i)} \cdot \Phi^{-1} \circ U_\ell^{(i,j)}$$

in (10), where $\Phi^{-1} \circ U_\ell^{(i,j)}$ denotes the application of Φ^{-1} to every component of $U_\ell^{(i,j)}$, we obtain a random bit counterpart to W_ℓ .

Next, we turn to the Brownian increments, and we put

$$\Delta_{k,\ell}^{(i,j)} = s^{(i,j)}(t_{k,\ell}) - s^{(i,j)}(t_{k-1,\ell}).$$

We use (2) with

$$V_{k,\ell} = \Delta_{k,\ell}^{(0,1)} \cdot Y_\ell^{(0,1)} + \sum_{i=1}^{\ell} \sum_{j=1}^{2^{i-1}} \Delta_{k,\ell}^{(i,j)} \cdot Y_\ell^{(i,j)}$$

to approximate, in distribution, the Brownian increments corresponding to (1).

Lemma 1. *The components of $V_{k,\ell}$ have mean zero and variance $2^{-\ell}$.*

The normalization is crucial in the definition of the random vectors $Y_\ell^{(i,j)}$. In fact, without this normalization the variances of the Brownian increments are not even matched asymptotically, and thus one can not expect the Euler scheme to converge, in any reasonable sense, to the true solution of the SDE.

Lemma 2. *The components of*

$$V'_{k,\ell} = \Delta_{k,\ell}^{(0,1)} \cdot \Phi^{-1} \circ U_\ell^{(0,1)} + \sum_{i=1}^{\ell} \sum_{j=1}^{2^{i-1}} \Delta_{k,\ell}^{(i,j)} \cdot \Phi^{-1} \circ U_\ell^{(i,j)}$$

have mean zero and variance at most $0.9 \cdot 2^{-\ell}$ for $\ell \geq 1$.

See the Appendix for the proofs of Lemma 1 and Lemma 2.

Let $\ell \geq 1$. For the multilevel construction we have to couple V_ℓ in a suitable way to a random vector $\tilde{V}_{\ell-1}$ that approximates, in distribution, the Brownian increments with step-size $2^{-(\ell-1)}$. To this end we introduce the rounding function

$$T_q: [0, 1[\rightarrow D_q, \quad x \mapsto \frac{\lfloor 2^q x \rfloor}{2^q} + 2^{-(q+1)},$$

see (8), and we put

$$T_{\ell-1}^{(i)} = T_{q_{\ell-1}^{(i)}}$$

for $i = 0, \dots, \ell - 1$ to obtain

$$(12) \quad U_{\ell-1}^{(i,j)} \stackrel{d}{=} T_{\ell-1}^{(i)} \circ U_\ell^{(i,j)}$$

for $j = 1$ if $i = 0$ and for $j = 1, \dots, 2^{i-1}$ if $i \geq 1$. We define

$$\tilde{Y}_{\ell-1}^{(i,j)} = 1/\sigma_{\ell-1}^{(i)} \cdot \Phi^{-1} \circ T_{\ell-1}^{(i)} \circ U_\ell^{(i,j)},$$

and we use (4) with

$$\tilde{V}_{k,\ell-1} = \Delta_{k,\ell-1}^{(0,1)} \cdot \tilde{Y}_{\ell-1}^{(0,1)} + \sum_{i=1}^{\ell-1} \sum_{j=1}^{2^{i-1}} \Delta_{k,\ell-1}^{(i,j)} \cdot \tilde{Y}_{\ell-1}^{(i,j)}.$$

Observe that $q_\ell^{(i)} - q_{\ell-1}^{(i)} = 2$. Hence $\tilde{V}_{\ell-1}$ is, roughly speaking, obtained from V_ℓ by ignoring the two least important bits in all of the relevant terms.

We stress that neither V_ℓ nor $\tilde{V}_{\ell-1}$ has independent components, except for the trivial cases $\ell = 0$ or $\ell = 1$, respectively, so that (i) is not satisfied. On the other hand, (12) implies that we have matching distributions in the sense of (ii).

The number of random bits that are needed to simulate the distribution of V_ℓ with $\ell = 0$ or the joint distribution of V_ℓ and $\tilde{V}_{\ell-1}$ with $\ell \geq 1$ is given by

$$d \cdot \left(q_\ell^{(0)} + \sum_{i=1}^{\ell} 2^{i-1} \cdot q_\ell^{(i)} \right) = d \cdot (2^{\ell+2} - 2),$$

which is easily verified by induction, cf. [7, Thm. 2]. Furthermore, the arithmetic cost to compute V_ℓ , together with $\tilde{V}_{\ell-1}$ if $\ell \geq 1$, is of the order $d \cdot 2^\ell$, see, e.g., [10, Sec. 2.2].

Let us discuss two important differences between the two constructions from [1, 6], which have been discussed in Section 2.2, and the construction based on the Lévy-Ciesielski representation.

The maximal level L has to be known in advance for the former two constructions, see (7) and (9), while this is not the case for the latter construction. Due to this difference the Lévy-Ciesielski based construction is well suited as the building block for an adaptive multilevel algorithm.

On the other hand, analytic results are only available for the constructions from [1, 6], since we have (i) and its analogon for $\tilde{V}_{\ell-1}$ only in these two cases.

3. ADAPTIVE ALGORITHMS AND EXPERIMENTS

We consider an adaptive multilevel algorithm with either one of the following building blocks:

- (1) The random bit Euler schemes with V_ℓ and \tilde{V}_ℓ based on the Lévy-Ciesielski representation, see Section 2.3. Notation: X_ℓ^{bit} and $\tilde{X}_{\ell-1}^{\text{bit}}$.
- (2) The classical Euler schemes with V_ℓ and \tilde{V}_ℓ based on the Brownian increments, see Section 2.1. Notation: X_ℓ^c and $\tilde{X}_{\ell-1}^c$.

The number of calls to the random number generator as well as the number of arithmetic operations to jointly simulate X_ℓ^* and $\tilde{X}_{\ell-1}^*$ with $\ell \geq 1$ is of the order 2^ℓ for both variants.

In both cases we use the adaptive algorithm A_ε^* from [5]. Here $\varepsilon > 0$ is an accuracy demand and input to the algorithm, and the maximal level as well as the replication numbers per level are determined adaptively.

We present numerical results for three different scalar SDEs, i.e., $r = d = 1$, where the solutions $E(f(X))$ are known analytically. For a fixed SDE and a fixed functional f we put

$$\text{bias}_\ell^* = E(f(X_\ell^*) - f(X_{\ell-1}^*))$$

and

$$\text{var}_\ell^* = \text{Var}(f(X_\ell^*) - f(X_{\ell-1}^*))$$

for $\ell \geq 1$. As key quantities we consider the root mean squared error

$$\text{rmse}_\varepsilon^* = \left(E(A_\varepsilon^*(f) - E(f(X)))^2 \right)^{1/2}$$

of A_ε^* , applied to f for the particular SDE, and the corresponding cost

$$\text{cost}_\varepsilon^* = E(C_\varepsilon^*(f)),$$

where $C_\varepsilon^*(f)$ denotes the number of calls of the random number generator for $\varepsilon > 0$. All of these quantities can be approximated by simple Monte Carlo algorithms, and the corresponding results will be presented together with asymptotic confidence intervals with confidence level 0.95 in the sequel. The number of Monte Carlo replications for the data points and confidence intervals involving root mean squared errors varies between $2 \cdot 10^3$ and $2 \cdot 10^4$.

3.1. Geometric Brownian Motion.

Here we consider the geometric Brownian motion X that solves

$$dX(t) = 1/50 \cdot X(t) dt + 1/5 \cdot X(t) dW(t), \quad t \in [0, 1],$$

with initial value $x_0 = 1$, as well as the path-dependent functional given by

$$f(x) = \max_{0 \leq t \leq 1} x(t).$$

Since $X(t) = \exp(W(t)/5)$, we obtain

$$E(f(X)) = E(\exp(|W(1)|/5)) = (2/\pi)^{1/2} \cdot \int_0^\infty \exp(y/5 - y^2/2) dy = 1.1819 \dots$$

At first we compare the random bit Euler scheme X_ℓ^{bit} and the classical Euler scheme X_ℓ^c in terms of their bias and variance, see Figure 1. Since f is Lipschitz continuous w.r.t. the supremum norm on $C([0, 1])$, we have the well-known upper bound

$$\text{var}_\ell^c = O(\ell \cdot 2^{-\ell})$$

and, consequently,

$$|\text{bias}_\ell^c| = O\left(\ell^{1/2} \cdot 2^{-\ell/2}\right).$$

These upper bounds are very well reflected in the actual bias and variance decays, and we observe no essential difference between the random bit and the classical Euler scheme.

Next we compare the multilevel algorithms $A_\varepsilon^{\text{bit}}$ and A_ε^c . At first we relate the root mean squared error $\text{rmse}_\varepsilon^*$ to the accuracy demand ε , see Figure 2, where we consider 25 different values of ε in a reasonable range. For both algorithms the root mean squared error is almost equal to the accuracy demand.

Finally we relate $\text{cost}_\varepsilon^*$ to the root mean squared error $\text{rmse}_\varepsilon^*$, see Figure 3, which is based on the same data set as Figure 2. We add that the confidence intervals for $\text{cost}_\varepsilon^*$ in Figure 3 are rather small and hardly visible. Figure 3 includes two graphs of functions $\varepsilon \mapsto \kappa \cdot \varepsilon^{-2} \cdot (\ln(\varepsilon^{-1}))^\gamma$ with parameters $\kappa > 0$

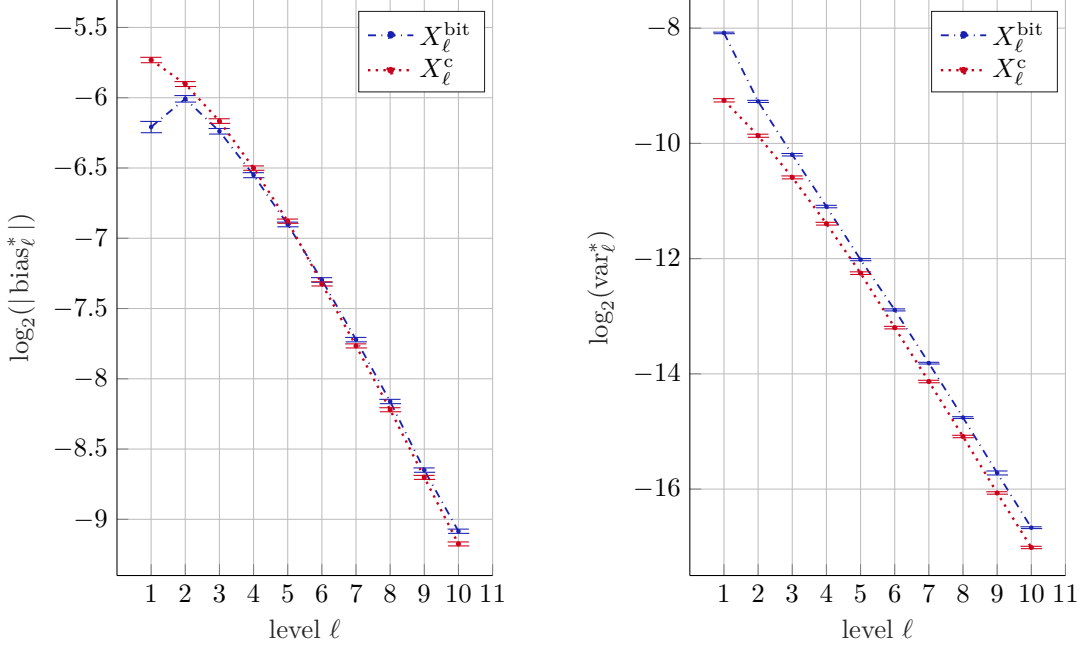


FIGURE 1. Maximum of a geometric Brownian motion: bias and variance vs. level

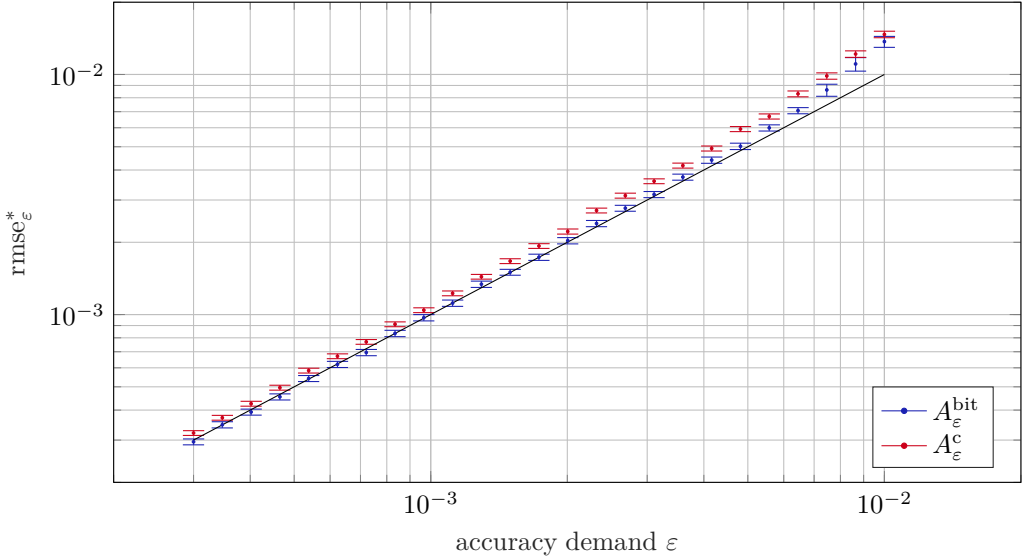


FIGURE 2. Maximum of a geometric Brownian motion: root mean squared error vs. accuracy demand

and $\gamma \in \mathbb{R}$, which are fitted to the respective data by hand. We obtain a log-exponent of $\gamma = 1.6$ as a good fit for both algorithms. The presence of a logarithmic term, i.e., $\gamma \neq 0$, corresponds to the actual bias and variance decays. The number of random bits is roughly $\kappa^{\text{bit}}/\kappa^{\text{c}} = 4.57$ times larger than the number of random numbers for the same root mean squared error.

3.2. Ornstein-Uhlenbeck Process. Here we consider the Ornstein-Uhlenbeck process X that solves

$$dX(t) = (2 - X(t)) dt + dW(t), \quad t \in [0, 1],$$

with initial value $x_0 = 1$, as well as the path-independent functional given by

$$(13) \quad f(x) = x(1).$$

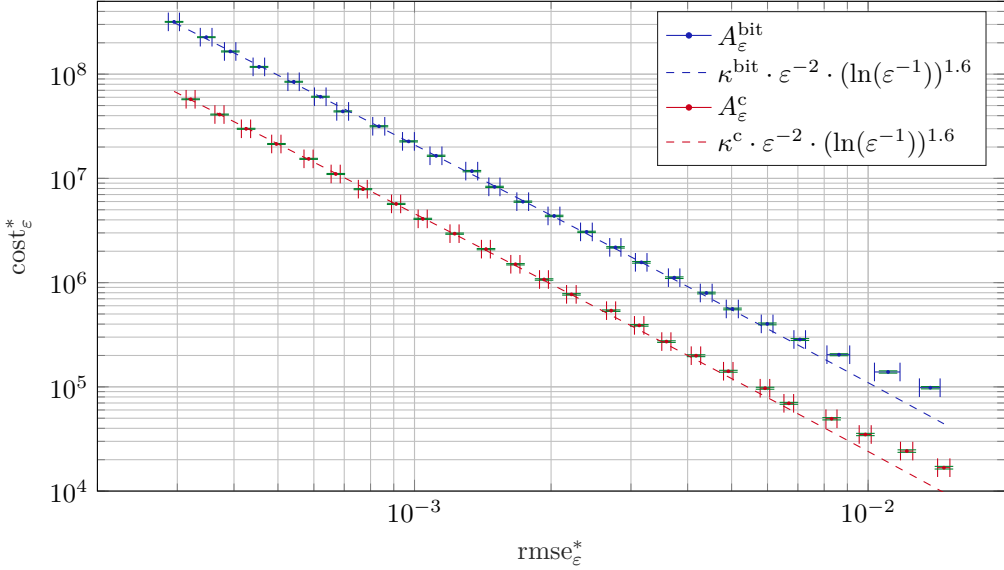


FIGURE 3. Maximum of a geometric Brownian motion: cost vs. root mean squared error

Since $X(t) = \exp(-t) + 2(1 - \exp(-t)) + \int_0^t \exp(-(t-s)) dW_s$, we obtain

$$E(f(X)) = 2 - \exp(-1) = 1.6321 \dots$$

As a major difference to the previous example we have improved upper bounds for the classical Euler scheme X_ℓ^c , namely,

$$(14) \quad \text{var}_\ell^c = O(2^{-2\ell})$$

and, consequently,

$$(15) \quad |\text{bias}_\ell^c| = O(2^{-\ell}).$$

For the numerical experiments we proceed as in the previous section. As for the geometric Brownian motion, the upper bounds (14) and (15) are very well reflected in the actual bias and variance decays, and we observe no essential difference between the random bit and the classical Euler scheme, see Figure 4.

For both multilevel algorithms the root mean squared error is again almost equal to the accuracy demand, see Figure 5.

Due to the improved upper bounds for the variance and bias it is natural to expect that cost_ℓ^* is proportional to $(\text{rmse}_\ell^*)^{-2}$. This is in line with the numerical results in Figure 6. Furthermore, we have $\kappa^{\text{bit}}/\kappa^c = 6.85$.

3.3. Cox-Ingersoll-Ross Process. Here we consider the Cox-Ingersoll-Ross process X that solves

$$dX(t) = (3/2 - X(t)) dt + 2 \cdot \sqrt{X(t)} dW(t), \quad t \in [0, 1],$$

with initial value $x_0 = 1$, as well as f given by (13). We have

$$E(f(X)) = \exp(-1) + \frac{3}{2}(1 - \exp(-1)) = 1.3160 \dots,$$

see, e.g., [3, Eqn. (19)]. To get a well-defined variant of the Euler scheme we take the positive part in every Euler step, i.e., we take the maximum with 0 of the right-hand side in (3) and (5).

Furthermore, we compare this Euler scheme with a truncated Milstein scheme, which is proposed and analyzed in [9]. For this scheme the right-hand side of (3), and similarly also for (5), is replaced by $\Theta_{\text{tMil}}(X_\ell(t_{k-1, \ell}), 2^{-\ell}, V_{k, \ell})$, where

$$\Theta_{\text{tMil}}(x, h, w) = \max \left(0, \left(\max \left(\sqrt{h}, \sqrt{\max(h, x)} + w \right) \right)^2 + (1/2 - x) \cdot h \right).$$

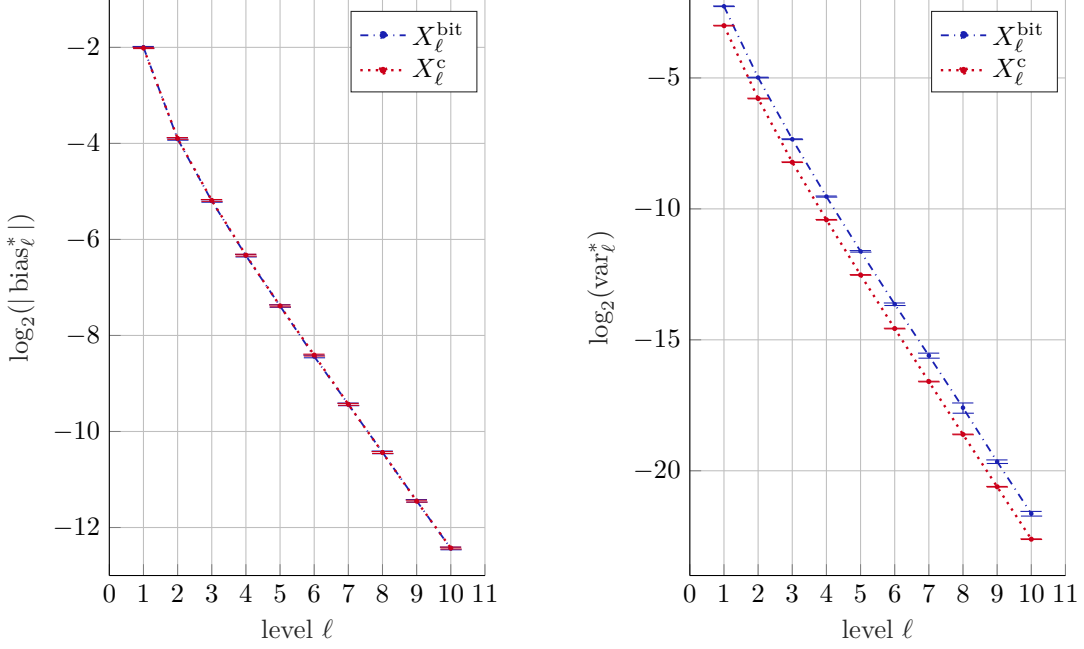


FIGURE 4. Ornstein-Uhlenbeck process at final time: bias and variance vs. level

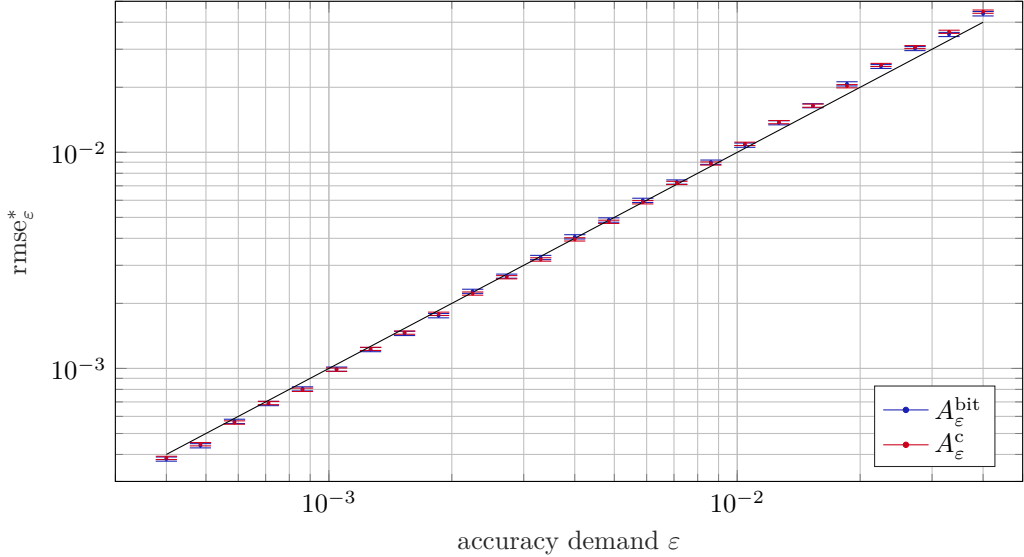


FIGURE 5. Ornstein-Uhlenbeck process at final time: root mean squared error vs. accuracy demand

The resulting schemes are denoted by $X_\ell^{\text{c,tMil}}$ and $X_\ell^{\text{bit,tMil}}$. For the Euler scheme no polynomial strong convergence rate is known. For the truncated Milstein scheme the strong convergence result from [9, Thm. 1] implies

$$(16) \quad \text{var}_\ell^{\text{c,tMil}} = O\left(2^{-\ell/2+\varepsilon\cdot\ell}\right)$$

and

$$(17) \quad |\text{bias}_\ell^{\text{c,tMil}}| = O\left(2^{-\ell/2+\varepsilon\cdot\ell}\right)$$

for every $\varepsilon > 0$. This strong convergence rate is the best known convergence rate for the Cox-Ingersoll-Ross process, see [8, Fig. 1.1].

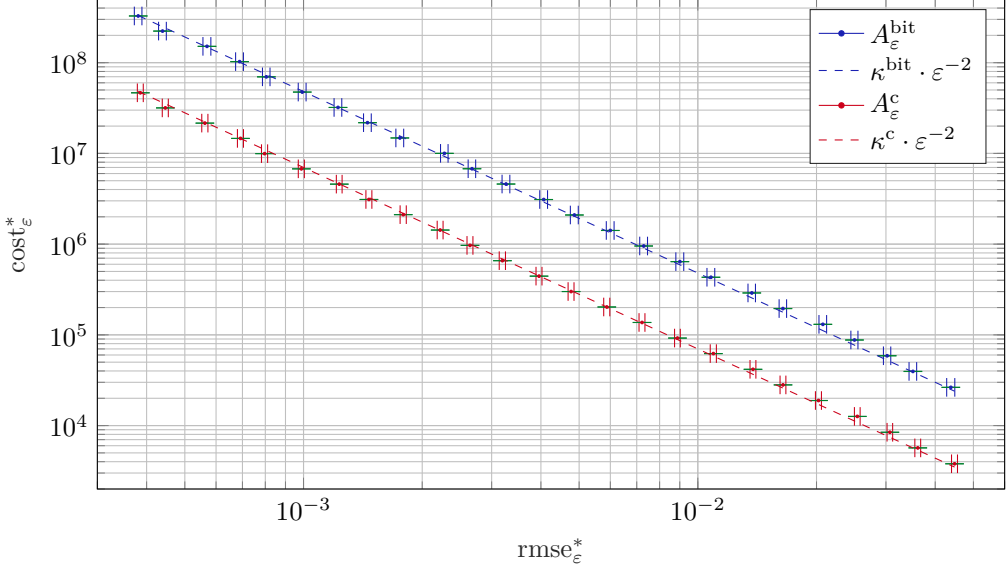


FIGURE 6. Ornstein-Uhlenbeck process at final time: cost vs. root mean squared error

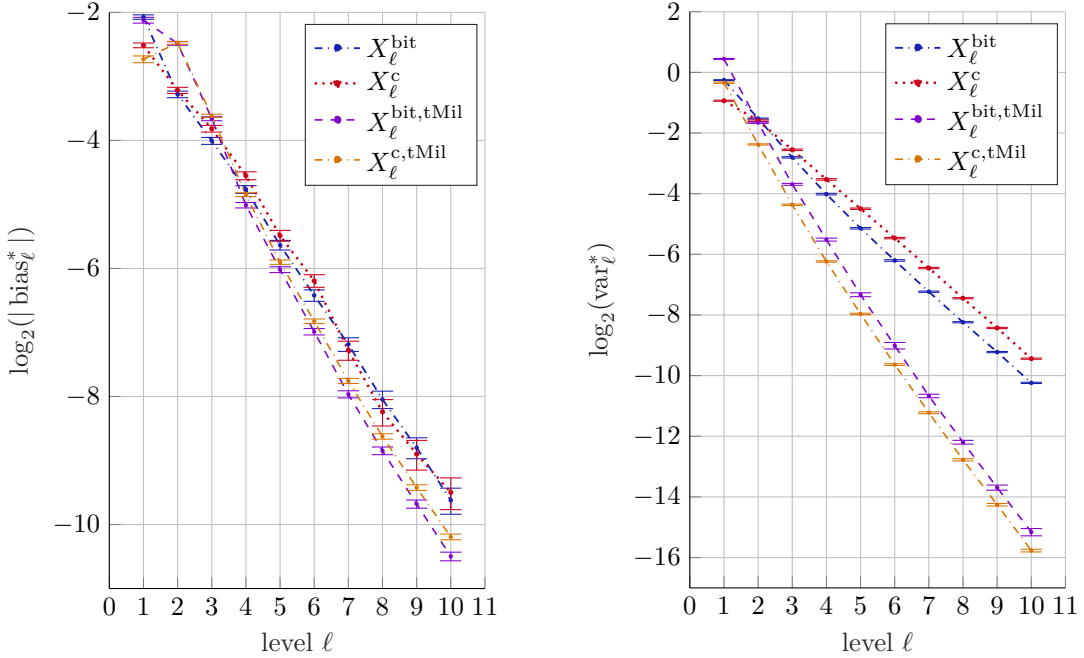


FIGURE 7. Cox-Ingerson-Ross process at final time: bias and variance vs. level

For the numerical experiments we proceed as in the previous sections. The decay of the bias for all four variants is similar to the decay of the bias for the Ornstein-Uhlenbeck process. The decay of the variance for both variants based on the Euler scheme is similar to the decay of the variance for the geometric Brownian motion. The decay of the variance for both versions based on the truncated Milstein scheme is similar and substantially faster. Note that the upper bounds (16) and (17) seem to be too pessimistic, cf. the conjecture in [9, Fig. 5].

For all four algorithms the root mean squared error is almost equal to the accuracy demand, see Figure 8, as is the case of the SDEs considered before.

Finally we relate $\text{cost}_\varepsilon^*$ to the root mean squared error $\text{rmse}_\varepsilon^*$, see Figure 9. The exponent γ of the logarithmic term is equal to 1.2 for both variants that are based on the Euler scheme and equal to 0.5 for both variants that are based on the truncated Milstein scheme. The better log-exponent corresponds

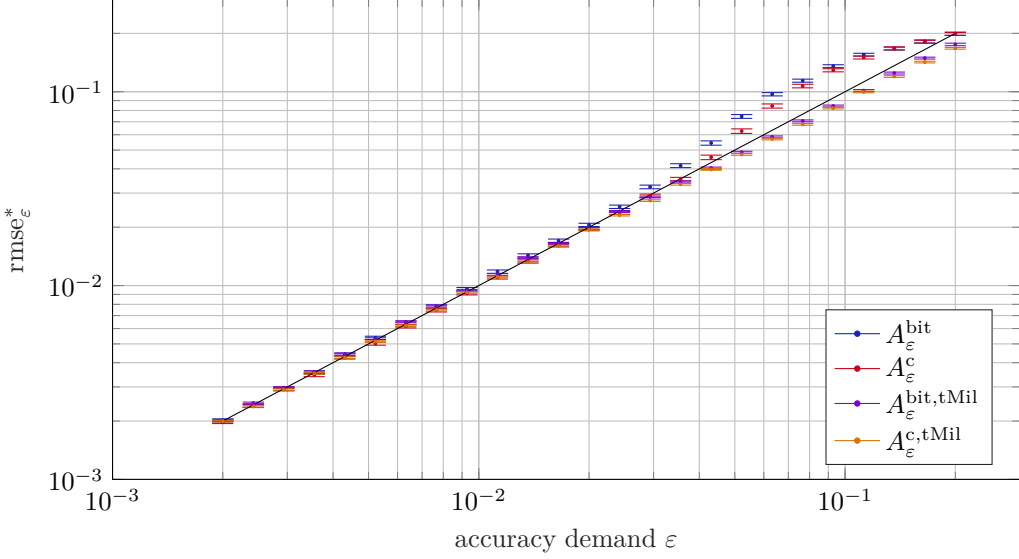


FIGURE 8. Cox-Ingersoll-Ross process at final time: root mean squared error vs. accuracy demand ε

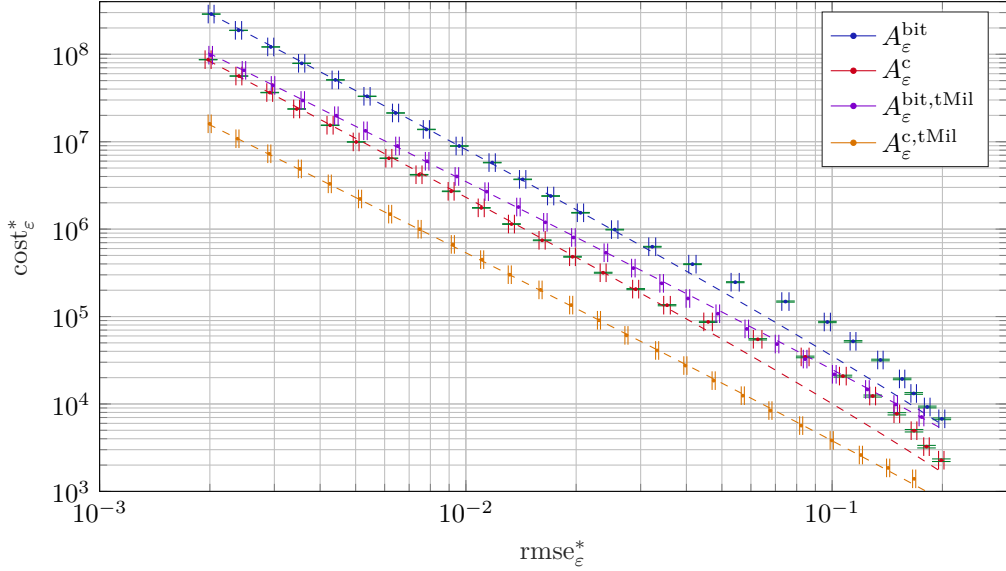


FIGURE 9. Cox-Ingersoll-Ross process at final time: cost vs. root mean squared error

to the faster decay of the variances. Furthermore, we have $\kappa^{\text{bit}}/\kappa^{\text{c}} = 3.51$ and $\kappa^{\text{bit,tMil}}/\kappa^{\text{c,tMil}} = 6.52$, and the multilevel algorithm based on the Euler scheme with random numbers has roughly the same root mean squared error as the multilevel algorithm based on the truncated Milstein scheme using random bits in the range considered in Figure 9.

ACKNOWLEDGEMENT

Mike Giles was partially supported by the UK Engineering and Physical Science Research Council (EPSRC) through the ICONIC Programme Grant, EP/P020720/1. Lukas Mayer was supported by the Deutsche Forschungsgemeinschaft (DFG) within the RTG 1932 ‘Stochastic Models for Innovations in the Engineering Sciences’.

APPENDIX

We present the proofs of Lemma 1 and Lemma 2. For notational convenience we consider the case $d = 1$. Recall that $Z^{(0,1)}, \dots, Z^{(\ell, 2^{\ell-1})}$ are independent and standard normally distributed.

The distribution of $U_\ell^{(i,j)}$ is symmetric with respect to 1/2, so that $E(Y_\ell^{(i,j)}) = 0$. Moreover, we have $\text{Var}(Y_\ell^{(i,j)}) = 1$ by construction. It follows that $E(V_{k,\ell}) = 0$ and

$$\begin{aligned} \text{Var}(V_{k,\ell}) &= (\Delta_{k,\ell}^{(0,1)})^2 + \sum_{i=1}^{\ell} \sum_{j=1}^{2^{i-1}} (\Delta_{k,\ell}^{(i,j)})^2 \\ &= \text{Var}\left(\Delta_{k,\ell}^{(0,1)} \cdot Z^{(0,1)} + \sum_{i=1}^{\ell} \sum_{j=1}^{2^{i-1}} \Delta_{k,\ell}^{(i,j)} \cdot Z^{(i,j)}\right) \\ &= \text{Var}(W_\ell(t_{k,\ell}) - W_\ell(t_{k-1,\ell})) = 2^{-\ell} \end{aligned}$$

due to (11) and the convergence of the Lévy-Ciesielski representation.

We have

$$\text{Var}(\Phi^{-1} \circ U_\ell^{(i,j)}) \leq 1,$$

see the end of the proof of [7, Thm. 1], and in particular for $i = \ell$

$$\text{Var}(\Phi^{-1} \circ U_\ell^{(\ell,j)}) \leq 4/5,$$

which follows from a simple computation. It follows that

$$\begin{aligned} \text{Var}(V'_{k,\ell}) &= (\Delta_{k,\ell}^{(0,1)})^2 \cdot \text{Var}(\Phi^{-1} \circ U_\ell^{(0,1)}) + \sum_{i=1}^{\ell} \sum_{j=1}^{2^{i-1}} (\Delta_{k,\ell}^{(i,j)})^2 \cdot \text{Var}(\Phi^{-1} \circ U_\ell^{(i,j)}) \\ &\leq (\Delta_{k,\ell}^{(0,1)})^2 + \sum_{i=1}^{\ell-1} \sum_{j=1}^{2^{i-1}} (\Delta_{k,\ell}^{(i,j)})^2 + \sum_{j=1}^{2^{\ell-1}} (\Delta_{k,\ell}^{(\ell,j)})^2 \cdot \text{Var}(\Phi^{-1} \circ U_\ell^{(\ell,j)}) \\ &\leq 2^{-\ell} - \sum_{j=1}^{2^{\ell-1}} (\Delta_{k,\ell}^{(\ell,j)})^2 \cdot (1 - \text{Var}(\Phi^{-1} \circ U_\ell^{(\ell,j)})) \\ &\leq 2^{-\ell} - 1/5 \cdot \sum_{j=1}^{2^{\ell-1}} (\Delta_{k,\ell}^{(\ell,j)})^2 = 9/10 \cdot 2^{-\ell}. \end{aligned}$$

REFERENCES

- [1] Denis Belomestny and Tigran Nagapetyan. Multilevel path simulation for weak approximation schemes with application to Lévy-driven SDEs. *Bernoulli*, 23(2):927–950, 2017.
- [2] C. Brugger, C. De Schryver, N. Wehn, S. Omland, M. Hefter, K. Ritter, A. Kostiuk, and R. Korn. Mixed precision multilevel Monte Carlo on hybrid computing systems. In *2014 IEEE Conference on Computational Intelligence for Financial Engineering Economics (CIFEr)*, pages 215–222, March 2014.
- [3] John C. Cox, Jonathan E. Ingersoll, Jr., and Stephen A. Ross. A theory of the term structure of interest rates. *Econometrica*, 53(2):385–407, 1985.
- [4] Michael B. Giles. Multilevel Monte Carlo methods. *Acta Numer.*, 24:259–328, 2015.
- [5] Michael B. Giles. Multilevel Monte Carlo software. <http://people.maths.ox.ac.uk/~gilesml/mlmc>, accessed: Jan. 2019.
- [6] Michael B. Giles, Mario Hefter, Lukas Mayer, and Klaus Ritter. Random bit multilevel algorithms for stochastic differential equations. *J. Complexity*, 2019. In press.
- [7] Michael B. Giles, Mario Hefter, Lukas Mayer, and Klaus Ritter. Random bit quadrature and approximation of distributions on Hilbert spaces. *Found. Comput. Math.*, 19(1):205–238, 2019.
- [8] Mario Hefter and André Herzwurm. Optimal strong approximation of the one-dimensional squared Bessel process. *Commun. Math. Sci.*, 15(8):2121–2141, 2017.
- [9] Mario Hefter and André Herzwurm. Strong convergence rates for Cox-Ingersoll-Ross processes — Full parameter range. *J. Math. Anal. Appl.*, 459(2):1079–1101, 2018.
- [10] Gunther Leobacher. Fast orthogonal transforms and generation of Brownian paths. *J. Complexity*, 28(2):278–302, 2012.
- [11] S. Omland, M. Hefter, K. Ritter, C. Brugger, C. De Schryver, N. Wehn, and A. Kostiuk. Exploiting mixed-precision arithmetics in a multilevel Monte Carlo approach on FPGAs. In C. De Schryver, editor, *FPGA Based Accelerators for Financial Applications*, pages 191–220. Springer, 2015.

[12] Steffen Omland. *Mixed Precision Multilevel Monte Carlo Algorithms for Reconfigurable Hardware Systems*. PhD thesis, Technische Universität Kaiserslautern, 2016.

MATHEMATICAL INSTITUTE, UNIVERSITY OF OXFORD, OXFORD OX2 6GG, ENGLAND
E-mail address: mike.giles@maths.ox.ac.uk

FACHBEREICH MATHEMATIK, TECHNISCHE UNIVERSITÄT Kaiserslautern, POSTFACH 3049, 67653 Kaiserslautern, GERMANY
E-mail address: {hefter, lmayer, ritter}@mathematik.uni-kl.de